ERROR ANALYSIS IN THE JOINT EVENT LOCATION/SEISMIC CALIBRATION INVERSE PROBLEM

William L. Rodi

Massachusetts Institute of Technology

Sponsored by Air Force Research Laboratory

Contract No. F19628-03-C-0109

ABSTRACT

It is well established that errors in global travel-time models can induce large biases into event locations inferred from regional and teleseismic arrival-time observations. Conversely, the travel-time corrections to these models that are estimated from calibration arrival times are affected by errors in the locations of the ground-truth events providing the data. This project addresses the interaction between location and calibration uncertainty in the context of the joint location/calibration inverse problem, in which arrival time data from multiple events and stations are used to simultaneously determine the locations of the events and calibration parameters such as 3-D velocity models or explicit path corrections. The project builds on and integrates mathematical and computational techniques developed in previous projects, including a grid-search algorithm for multiple-event location, a Monte Carlo technique for location uncertainty analysis, and a new kriging method for empirical calibration. The ultimate goal is a procedure for computing accurate confidence regions on the locations of new events, reflecting the observational errors in their arrival-time data as well as the uncertainty inherited from incomplete and imperfect calibration data sets. This paper describes our formulation of the joint location/calibration inverse problem and the algorithm we have developed to date for performing a fully nonlinear location/calibration uncertainty analysis in the special case in which correction parameters comprise a simple time term for each seismic station and phase, as is often assumed in multiple-event location methods. We present initial applications of the algorithm to earthquake clusters in Turkey and nuclear explosions at the Nevada Test Site, for which very precise ground-truth locations are available for validation purposes. The results show the expected dependence of the location confidence region for an event on the ground-truth location constraints imposed on other events, thus confirming the concept of our new approach to event location uncertainty. The algorithm is computationally intensive, however, and we are investigating computational shortcuts and approximations that yield the same results more efficiently before extending the approach to more general parameterizations of travel-time corrections.

OBJECTIVE

The objective of this project is to develop new mathematical and computational techniques for quantifying the errors in seismic event locations, including the effects of observational errors and calibration errors, that is, errors in the travel-time forward model. Calibration errors stem from observational errors in calibration data, incomplete geographical coverage of these data, and uncertainty in the locations of the ground-truth events providing the data. Our goal is to take all of these error sources into account in determining the location uncertainty on new events.

Our approach to location uncertainty is formulated within the framework of the joint location/calibration inverse problem. In this problem, arrival time data from multiple events and stations are used to simultaneously determine the event locations and calibration parameters, such as explicit path corrections or a 3-D velocity model. We treat one of the events as a new event under investigation and the remaining events as calibration events. A complete error analysis that considers the uncertainty in all the unknown parameters—the location of the new event, the locations of non-GT0 calibration events, and the calibration parameters—accounts for the sources of location uncertainty, which are the topic of this project.

We are addressing this joint inverse problem with numerical techniques that lift key limitations in previous analytic approaches to uncertainty analysis in large inverse problems. These limitations include the restriction to Gaussian data errors, the necessity of using a linear approximation to the forward model, and restricted mechanisms for incorporating *a priori* constraints on the unknowns. Hard bounds on parameters, in particular, are not accommodated in the analytical approach and these can introduce a nonlinearity to the problem that can be more severe than the nonlinearity of the forward model. Requiring an event location to be below the Earth's surface is an example of such a constraint. The primary numerical methods we are currently using to accommodate these complexities are grid search, for finding optimal solutions for parameters, and Monte Carlo sampling, for finding confidence regions on parameters.

Given the ability to perform a rigorous analysis of event location uncertainty, the ultimate objective of this project is to achieve a more complete understanding of the main factors controlling the errors in seismic locations and to identify the new information or procedures needed to reduce these errors for the purposes of improved nuclear-event monitoring.

RESEARCH ACCOMPLISHED

Formulation of the Joint Inverse Problem

We state our formulation of the joint location/calibration inverse problem for a data set comprising the arrival times of n seismic station/phase combinations (e.g. phase Pn at station MNV) observed from a subset of m seismic events. Let d_{ij} denote the observation for the ith event and jth station/phase (i,jth path). Then the joint event location/seismic calibration inverse problem can be written as

$$d_{ij} = t_i + T_j(\mathbf{x}_i) + c_{ij} + e_{ij} \tag{1}$$

where t_i and $\mathbf{x}_i$ are origin parameters (time and hypocenter, respectively) of the ith event; T_j is a model-based travel-time function for the jth station/phase; c_{ij} is a correction to this function; and e_{ij} is an observational error. This equation holds only for the paths i, j for which data have been observed.

The unknown parameters of this joint location/calibration inverse problem are the event hypocenters and origin times, $\mathbf{x}_i$, t_i, $i = 1,\ldots,m$, and the path travel-time corrections c_{ij}. The problem becomes one of purely calibration when the event parameters are assumed known, and one of purely location when the path corrections are known. In practice, neither set of parameters is completely known or unknown. Two difficult aspects of nuclear monitoring, in fact, fall within the general formulation. The first is how to account for uncertainty in a seismic calibration (errors in estimates of c_{ij}) when the calibration events have imperfectly known locations, i.e. ground-truth (GT) levels greater than zero. The second is how the location error of any particular event is affected by imperfect knowledge of the path corrections. These difficult questions are addressed by a complete uncertainty analysis in the joint location/calibration problem.

Parameterization of path corrections

The joint inverse problem is hopelessly ill-posed if the path corrections c_{ij} are not constrained via prior information or a parameterization that reduces the number of independent unknowns, or both. The exact nature of the inverse problem depends on how this is done.

In the "basic" multiple-event location problem, relevant to small event clusters, the path corrections are assumed to be event-independent, i.e.

$$c_{ij} = a_j. \tag{2}$$

The calibration parameters comprise a time term, a_j, for each station/phase pair in the data set. This problem has been treated by several workers (e.g. Jordan and Sverdrup, 1981; Pavlis and Booker, 1983) and it is the focus of this paper. However, our formulation pertains to other ways of parameterizing path corrections that will be addressed later in the project. One is with correction functions (or surfaces), whereby

$$c_{ij} = a_j\,(\mathbf{x}_i). \tag{3}$$

Here, there is an unknown function, $a_j\,(\mathbf{x})$, assigned to each station/phase. Another is the universal parameter function described by Rodi et al. (2003). Spatial functions contain many more degrees of freedom than simple time terms and it is necessary to provide prior information on their smoothness, such as with geo-statistical constraints (e.g. Schultz et al., 1998), to make the inverse problem well posed. Our formulation also includes the problem of earthquake tomography (joint location/velocity determination; e.g. Spencer and Gubbins, 1980) as a special case. Path corrections are then parameterized by the Earth's velocity function and the c_{ij} are integrations of this function over ray paths.

Maximum-likelihood formulation

Our approach to inverse problems and uncertainty analysis is based on likelihood functions. A likelihood function is a function of the unknown parameters whose purpose is to quantify how well any given values for the parameters agree with the observed data. An optimal estimate of the unknown parameters (the *maximum-likelihood* estimate) can be taken as those parameter values that maximize the likelihood function. A confidence region on the parameters is the collection of parameter values whose likelihood is within some tolerance of the maximum likelihood.

A given assumption about the probability distribution of the data errors defines a particular likelihood function for the parameters. In our work thus far we have assumed that the observational (picking) errors, e_{ij}, are statistically independent and that each has a *generalized Gaussian* probability distribution of order p (Billings et al., 1994). For the small-cluster problem ($c_{ij} = a_j$), this error model implies a likelihood function, L, given by

$$-\log L = \mathbf{const} + \sum_{ij} \log \sigma_{ij} + \frac{1}{p} \sum_{ij} \frac{1}{\left(\sigma_{ij}\right)^p} \left| d_{ij} - t_i - T_j\left(\mathbf{x}_i\right) - a_j \right|^p . \tag{4}$$

In this paper we will assume the data standard errors, σ_{ij}, are known *a priori*. The task of maximizing the likelihood is then equivalent to minimizing an L_p norm (to the pth power) of the data residuals, as given by the last term of equation (4). The case of Gaussian errors coincides with $p = 2$ and maximization of the likelihood function with respect to the problem unknowns (event locations and time terms) becomes a problem of nonlinear least squares.

In previous projects we have developed an algorithm called GMEL (grid-search multiple-event location) for maximizing the likelihood function in equation (4). The algorithm is described in Rodi et al. (2002). GMEL solves jointly for the location parameters of the events, $\mathbf{x}_i$ and t_i, and the travel-time correction terms of the station/phase combinations, a_j. It accepts prior constraints on all the parameters in the form of prior bounds. A prescribed lower and upper bound is allowed on each event origin time t_i, event depth z_i, and travel-time correction, a_j (e.g. $a_j^{\min} \le a_j \le a_j^{\max}$). Bounds on an event epicenter take the form of a maximum epicentral distance from a specified geographic point. The GMEL algorithm iterates over alternating loops over events, to update event locations with station/phase terms fixed, and over station/phase pairs, to update their correction terms with the event locations fixed. Grid search is used to find the optimal event locations.

Location Confidence Regions in the Joint Inverse Problem

Our formulation of uncertainty analysis in the joint location/calibration (or multiple-event location) inverse problem extends the formulation we developed for the single-event location problem (Rodi and Toksöz, 2001). The same principles are applied, but to a problem with many more parameters.

Our approach is to address the uncertainty in a subset of the unknown parameters, which we denote as a vector **p**, considering their trade-off with the remaining "hidden" parameters, **q**. For example, **p** may be the hypocenter of one of the events, say the first event ($\mathbf{p} = \mathbf{x}_1$). In single-event location, **q** would then be simply the origin time of the event ($\mathbf{q} = (t_1)$). In the multiple-event location problem, however, **q** includes this plus all the other event locations and the travel-time corrections:

$$\mathbf{q} = (t_1, \mathbf{x}_2, t_2, \ldots, \mathbf{x}_m, t_m, a_1, a_2, \ldots, a_n). \tag{5}$$

To address the uncertainty in the *epicenter* of event 1, as another example, we would move its depth, z_i, from **p** to **q**.

For single-event location, Flinn (1965) developed the methodology for hypocentral confidence regions for the case of Gaussian data errors ($p = 2$) and no parameter constraints, and using a linear approximation to the travel-time functions, T_j. His method can be formulated in terms of hypothesis testing using a likelihood ratio as the test statistic. Doing so allows us to define confidence regions under less restrictive assumptions and for the multiple-event problem.

In the multiple-event problem, let **d** denote the vector of arrival time data (d_{ij} for the observed *ij* pairs), and write the likelihood function as $L(\mathbf{p}, \mathbf{q}; \mathbf{d})$. We will denote the prior parameter constraints as sets P and Q, which contain the admissible values of **p** and **q**, respectively (e.g., for $\mathbf{p} = \mathbf{x}_1$, the below-surface constraint yields $\mathrm{P} = \{(\theta_1, \phi_1, z_1) \mid z_1 \geq 0\}$, where θ and ϕ are epicentral coordinates). A confidence region on **p** is defined in terms of a likelihood ratio test statistic, $\tau(\mathbf{p}, \mathbf{d})$, which compares the likelihoods that are achieved with **p** fixed to a particular value and with **p** free to vary within P. Thus

$$\tau(\mathbf{p}, \mathbf{d}) = \log \max_{\substack{\mathbf{p}' \in \mathrm{P} \\ \mathbf{q}' \in \mathrm{Q}}} L(\mathbf{p}', \mathbf{q}; \mathbf{d}) - \log \max_{\mathbf{q} \in \mathrm{Q}} L(\mathbf{p}, \mathbf{q}; \mathbf{d}). \tag{6}$$

Given a confidence level β, we can reject **p** at that level if $\tau(\mathbf{p}, \mathbf{d})$ is greater than some critical value, τ_β. This critical value is determined by the probability distribution of $\tau(\mathbf{p}, \mathbf{d})$, as induced by the errors in **d**. If **p** is *not* rejected, it is *inside* the confidence region for the specified confidence level. That is, the confidence region comprises the parameter vectors **p** satisfying

$$\tau(\mathbf{p}, \mathbf{d}) \leq \tau_\beta. \tag{7}$$

In Gaussian/linear inverse problems ("linear" means the T_j are linear *and* hard parameter constraints are not used), with the additional assumption that the standard errors (σ_{ij}) are known, τ (actually 2τ) is chi-squared distributed with the number of degrees of freedom being the number of parameters in **p** (e.g., 2 for epicentral confidence regions). Thus, τ_β is easily determined from tables of the chi-squared cumulative distribution function. Furthermore, in the Gaussian/linear case, the dependence of τ on **p** is quadratic. Therefore, the locus of points **p** satisfying equation (7) fill a hyper-ellipsoid whose axis lengths and orientations are easily found. With our more general assumptions (non-Gaussian errors, or nonlinear forward model or parameter constraints), τ does not necessarily have a well-known probability distribution and the geometry of a confidence region cannot be found with analytic formulas. Therefore, we use numerical techniques to find τ_β and the values of **p** that satisfy equation (7).

Confidence Region Algorithm

Our confidence region algorithm is a two-step procedure. We describe it for the case where **p** is the hypocenter, **x**, of one of the events, and where a single value of β is of interest (e.g. $\beta = 90\%$). The steps are

1. Compute $\tau(\mathbf{x}, \mathbf{d})$ at points $\mathbf{x}$ on a dense 3-D hypocenter grid. This entails maximizing L with respect to the hidden parameters ($\mathbf{q}$) for each $\mathbf{x}$ on the grid.
2. Perform a Monte Carlo simulation to find τ_β. This entails computing $\tau(\mathbf{x}^{tru}, \mathbf{d}^{syn})$ for an assumed "true" hypocenter $\mathbf{x}^{tru}$ and true hidden parameters $\mathbf{q}^{tru}$, and many realizations of synthetic data, $\mathbf{d}^{syn}$.

In step 2, each realization $\mathbf{d}^{syn}$ is constructed by adding a realization of pseudo-random errors to arrival times calculated for ($\mathbf{x}^{tru}$, $\mathbf{q}^{tru}$):

$$\mathbf{d}^{syn} = F(\mathbf{x}^{tru}, \mathbf{q}^{tru}) + \mathbf{e}^{syn} \tag{8}$$

where F denotes the arrival time forward model and $\mathbf{e}^{syn}$ is the pseudo-random noise vector (comprising the e_{ij}). The computation of $\tau(\mathbf{x}^{tru}, \mathbf{d}^{syn})$ requires that each realization of the synthetic data be used in two likelihood maximizations: one with $\mathbf{x} = \mathbf{x}^{tru}$ and one with $\mathbf{x}$ free to vary within its admissible region (X). Both maximizations vary $\mathbf{q} \in$ Q.

In our current implementation of this algorithm, we take $\mathbf{x}^{tru}$ and $\mathbf{q}^{tru}$ to be their maximum-likelihood values for the real data. The method then coincides with a statistical method called *parametric bootstrapping* (e.g. Hall, 1992).

Both steps of this procedure maximize the likelihood function many times. In step 1 (likelihood sampling) L is maximized for all hypocenters on a 3-D grid, but only for the real data. The second step (Monte Carlo simulation) entails maximizing L twice, with $\mathbf{x}$ fixed and free, for each of many realizations of synthetic data. (We have found that ~300 realizations of synthetic data yield stable results if β is not too close to 1.) In the single-event problem, maximizing L is a fast procedure and a confidence region can be computed with a few seconds of CPU time. In multiple-event location, each maximization of L is an invocation of the GMEL algorithm to solve for multiple event and station parameters. Even for *epicentral* confidence regions, with event depths assumed known (implying a 2-D sampling grid in step 1), each step of the procedure can require on the order of one hour of CPU time (on a 2.4 GHz Xeon processor), depending on the denseness of the epicenter sampling grid and the number of Monte Carlo realizations.

Other workers in event location uncertainty (c.f. Wilcock and Toomey, 1991) have used analytical values of τ_β in calculating location confidence regions, even while sampling the likelihood function (our algorithm step 1) to avoid linearization of the forward problem. Doing so avoids step 2 of our algorithm. For single-event location, we have performed numerical experiments with real and synthetic data to test the accuracy of analytical critical statistic values, in the case of Gaussian errors. We discovered that bounds on the target parameters $\mathbf{p}$ (e.g. depth bounds when computing hypocentral confidence regions) can lead to significant errors in the analytical τ_β. However, the experiments also showed that τ_β is not sensitive to the constraints on the *hidden* parameters, $\mathbf{q}$. For example, the statistic for an epicentral confidence region did not depend on whether or how strongly the focal depth was constrained.

This fact suggests a way to tremendously speed up the Monte Carlo simulation in the multiple-event problem: by fixing the locations of the calibration events (which are parameters in $\mathbf{q}$). In effect, single-event location is performed on each realization of synthetic data. We used this approximation in the applications below. We point out that the calibration events cannot be fixed for step 1 of the procedure, for doing so would ignore important trade-offs between the parameters in $\mathbf{p}$ and $\mathbf{q}$.

Application to the Izmit Earthquake Sequence

Rodi and Toksöz (2003) presented some preliminary tests of our multiple-event uncertainty approach applied to the 17 August 1999 Izmit, Turkey, earthquake sequence. These tests demonstrated the concept of the approach but revealed its computational difficulties. Here we present updated results for this data set, using finer sampling grids and more Monte Carlo realizations. The new results employ the approximation of fixing calibration event locations in the Monte Carlo simulation, as described in the previous section.

The data set previously used contains 3484 Pn and teleseismic P arrival times from 643 stations from the National Earthquake Information Center (NEIC), which we obtained from the IASPEI Working Group on Multiple-Event

Location, courtesy of R. Engdahl and E. Bergman. For the new tests we winnowed the data set by eliminating station/phase pairs having fewer than 3 events. The winnowed data subset comprises 3083 Pn or P arrivals from 373 stations (387 station/phase combinations) from 34 events (the Izmit mainshock and 33 aftershocks).

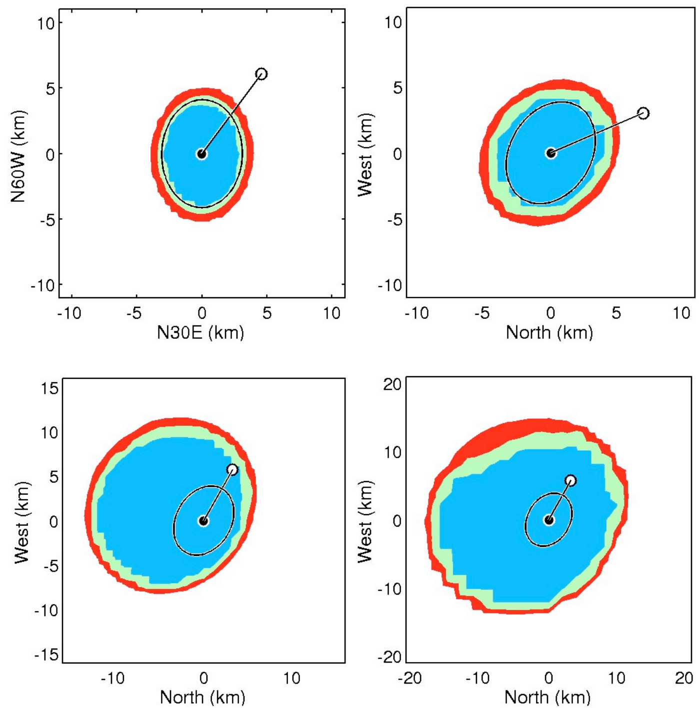

Figure 1. ***Top left*: Single-event epicentral confidence regions (at 90, 95 and 98% confidence; blue, green and red, respectively) for a well-recorded aftershock of the 1999 Izmit Turkey earthquake (135 defining phases). Station travel-time corrections were assumed to be known. *Top right and bottom left/right*: Multiple-event confidence regions for the same event. *Top right*: computed with the Izmit mainshock constrained as a GT0 event. *Bottom left*: with the Izmit mainshock constrained as a GT5 event. *Bottom right*: with the Izmit mainshock as a GT10 event. In each frame, the black circle marks the maximum-likelihood (GMEL) solution for the aftershock and the white circle is a GT5 local network solution for the event (Engdahl and Bergman, private communication). The ellipse is the analytic, single-event 90% confidence ellipse on the aftershock.**

We show confidence regions on two of the Izmit aftershocks. One is a well-recorded aftershock occurring on 31 August 1999, and has 135 defining phases in the winnowed data set (compared to 283 defining phases for the Izmit mainshock). The other is a poorly recorded aftershock on 26 August 1999 having 17 defining phases. Only epicentral confidence regions were calculated with depths fixed to values found by Engdahl and Bergman (2001). For both aftershocks, the Izmit mainshock was treated as a ground-truth calibration event. Its prior location was set to the solution from a local seismic network and is estimated to be of GT5 accuracy. In our tests, however, we assumed various GT levels of the mainshock. The other 32 “calibration” events were unconstrained. In all cases, picking errors were assumed to be Gaussian with a standard deviation of 0.622 sec. The AK135 travel-time tables were used for the forward model in all cases.

Figure 1 shows the confidence regions for the well-recorded aftershock. The top/left frame shows single-event confidence regions (at three confidence levels) found with our numerical approach. These assume the travel-time corrections are known exactly, making the calibration events irrelevant. The other three frames show multiple-event confidence regions, i.e. the corrections are assumed to be unknown and are only constrained by the calibration events with some degree of uncertainty. The multiple-event confidence regions were computed under the assumptions, respectively, that the Izmit mainshock was a GT0 event (upper right frame), a GT5 event (lower left) and GT10 event (lower right). In each frame, the maximum-likelihood location for the aftershock is compared to a GT5 local seismic solution that was available for the aftershock. Figure 2 shows the analogous computations for the poorly recorded aftershock.

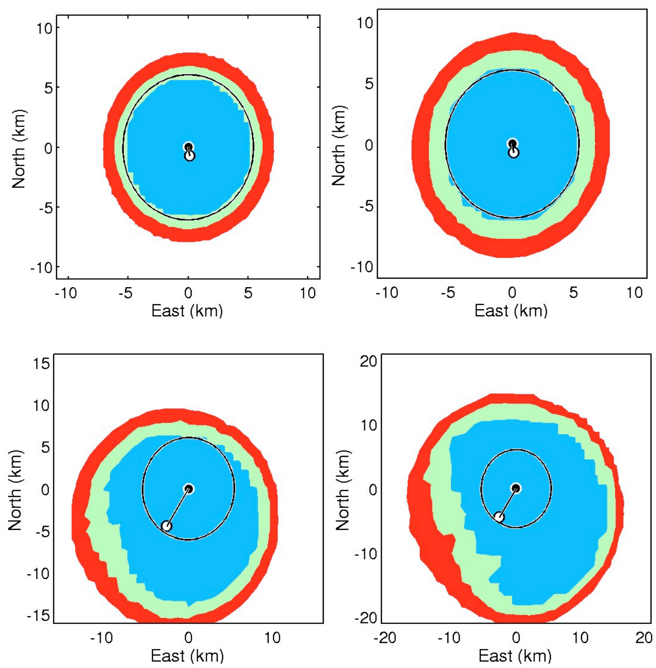

Figure 2. Same as Figure 1 but for a poorly recorded aftershock of the Izmit earthquake (17 defining phases).

The confidence regions in both figures show the behavior we expect. When the uncertainty in travel-time corrections is ignored (top left frames) the confidence regions are comparable to the confidence ellipses computed with the conventional Gaussian/linear formula (shown only for $\beta = 90\%$). When the uncertainty in corrections is accounted for (top right) the confidence regions are larger. When the GT level of the Izmit mainshock is increased (bottom frames) the regions become accordingly larger still. In the case of the well-recorded aftershock (Figure 1) only the bottom confidence regions, accounting for the location error in the one GT event, contain the local network solution.

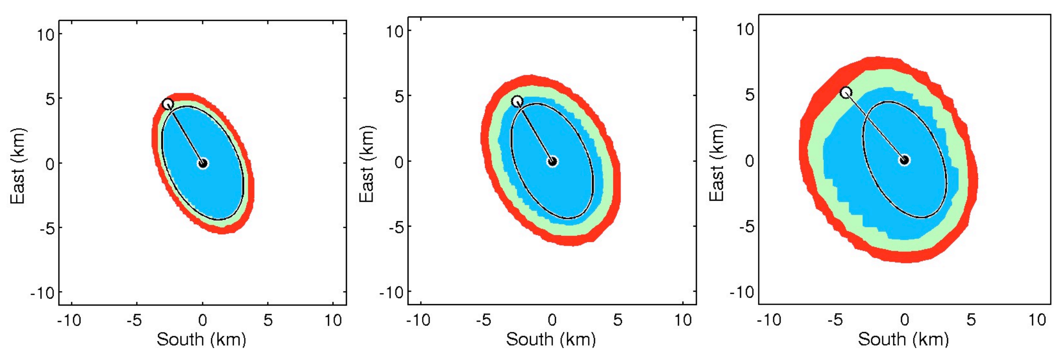

Figure 3. Epicenter confidence regions for a Rainier Mesa explosion determined from 6 Pn arrival times. *Left*: Single-event confidence regions (at 90, 95 and 98% confidence), computed with path travel-time corrections assumed known. *Center/Right*: Multiple-event confidence regions for the same event, allowing for the uncertainty in path corrections. *Center*: computed with one well-recorded Rainier Mesa explosion (22 Pn arrivals) constrained to be a GT0 event. *Right*: with the same explosion constrained as a GT2 event. All other events were unconstrained. In each frame the black circle marks the maximum-likelihood solution for the event and the white circle is its GT0 location (from Walter et al., 2003). The ellipse in each frame is the analytic, single-event 90% confidence ellipse on the event location.

Application to NTS Explosions

We have also tested our new error analysis technique on a data set from NTS explosions that has been assembled by Lawrence Livermore National Laboratory (LLNL) (Walter et al., 2003). The data set comprises 74 nuclear explosions with known locations and origin times recorded at a network of regional and local stations. The examples here use only a subset of the Pn picks from the data set, selected under the following criteria. First, arrivals from two stations (TPH and DAC) that are within 1.5° of most of the explosions were excluded, leaving only stations at greater distances. Of the remaining data set, events with fewer than 4 arrivals and stations with fewer than 2 arrivals were removed. The resulting subset comprises 548 arrivals from 71 events and 38 stations. IASP91 travel-time tables were used for the forward model. Picking errors were assumed to have a standard deviation of 0.324 sec.

The examples here follow the schema of the Izmit examples shown above. One NTS explosion was chosen as a ground-truth calibration event with finite GT level: GT0 or GT2 this time. This event was a Rainier Mesa explosion with 20 Pn arrivals. Several other events were treated, in turn, as new events to be located. The remaining 69 explosions in the winnowed data set were treated as calibration events with unconstrained locations.

Figures 3–6 show confidence regions on four of the explosions that have relatively few arrivals: one each from the Rainier Mesa and Pahute Mesa test areas and two from Yucca Flat. We see the same behavior of confidence regions as in the Izmit examples, with the regions growing as the uncertainty in travel-time corrections and the finite location accuracy of the GT calibration event are accounted for. We point out that the Rainier Mesa explosion was constrained with its GT0 location. Therefore, the confidence regions in the center frame of each figure should cover the GT0 location shown for the target event. In three of four cases, the GT0 location is near the edge of the confidence region and for one of the Yucca explosions it is decidedly outside the confidence region. Further study is needed to determine why this is the case, but a possible explanation is the inadequacy of a simple time-term parameterization of travel-time corrections.

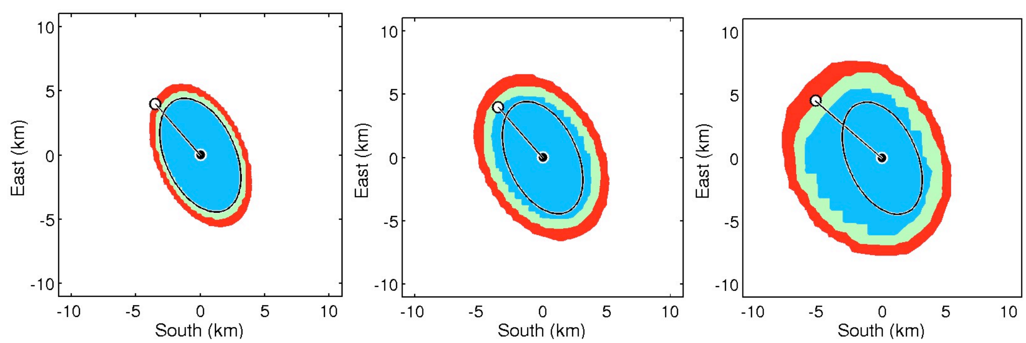

Figure 4. Epicenter confidence regions for a Pahute Mesa explosion determined from 6 Pn arrival times. See Figure 3 for explanation of the different frames and conventions.

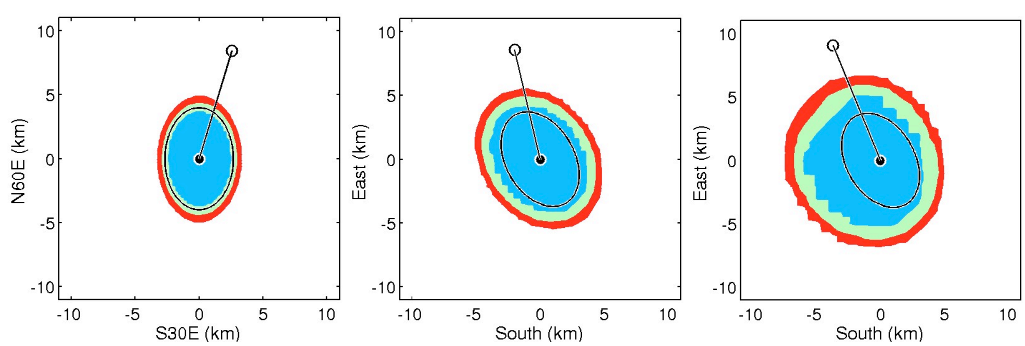

Figure 5. Epicenter confidence regions for a Yucca Flat explosion determined from 7 Pn arrival times. See Figure 3 for explanation of the different frames and conventions.

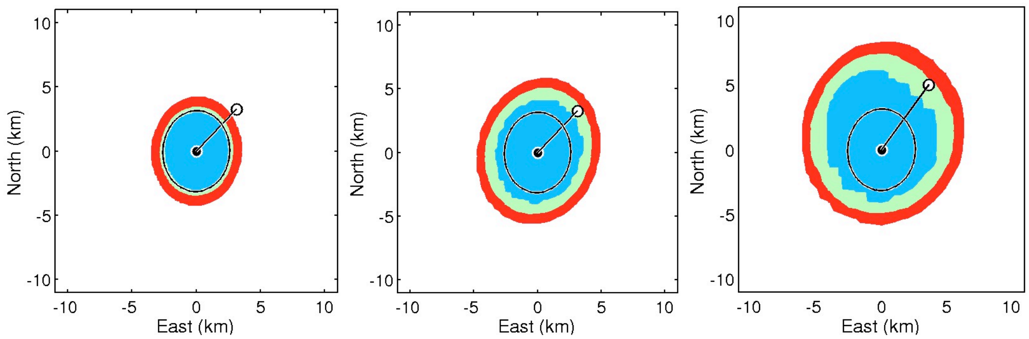

Figure 6. Epicenter confidence regions for a Yucca Flat explosion determined from 8 Pn arrival times. See Figure 3 for explanation of the different frames and conventions.

CONCLUSIONS AND RECOMMENDATIONS

We have developed a general theoretical and computational framework for characterizing the uncertainty in seismic event locations in the context of the joint inverse problem of multiple-event location and travel-time calibration. The approach accounts for complexities such as nonlinear forward models and parameter constraints and the finite accuracy of calibration event locations, which create significant difficulties for analytic methods of uncertainty analysis. We have implemented the approach for the basic multiple-event location problem with time-term corrections, and begun testing it with earthquake and explosion data sets. The results to date have validated the approach qualitatively but it awaits quantitative validation. We have made some significant inroads in improving the computational efficiency of the method. However, more improvement is needed for the method to be a tool of routine analysis, and if it is to be practical with more complex parameterizations of travel-time corrections.

ACKNOWLEDGMENTS

I wish to thank the people who provided the data used in this paper: Bob Engdahl and Eric Bergman of University of Colorado at Boulder, who provided the NEIC data for the Izmit earthquake sequence, and Steve Myers of Lawrence Livermore National Laboratory, who provided the NTS explosion data set.

REFERENCES

Billings, S.D., M.S. Sambridge and B.L.N. Kennett (1994). Errors in hypocenter location: picking, model and magnitude dependence, *Bull. Seism. Soc. Am., 84*, 1978-1990.

Engdahl, E.R. and E.A. Bergman (2001). Validation and generation of reference events by cluster analysis, *Proceedings*, 23rd Annual DoD/DOE Seismic Research Review, Jackson Hole, Wyoming.

Flinn, E.A. (1965). Confidence regions and error determinations for seismic event location, *Rev. Geophys., 3*, 157-185.

Hall, P. (1992). *The Bootstrap and Edgeworth Expansion*, Springer-Verlag, New York.

Jordan, T.H. and K.A. Sverdrup (1981). Teleseismic location techniques and their application to earthquake clusters in the south-central Pacific, *Bull. Seism. Soc. Am., 71*,1105-1130.

Myers, S.C. and C.A. Schultz (2000). Improving sparse network seismic locations with Bayesian kriging and teleseismically constrained calibration events, *Bull. Seism. Soc. Am., 90*, 199-211.

Pavlis, G.L. and J.R. Booker (1983). Progressive multiple event location (PMEL), *Bull. Seism. Soc. Am., 73*, 1753-1777.

Rodi, W. and M.N. Toksöz (2001). Uncertainty analysis in seismic event location, *Proceedings*, 23rd Annual DoD/DOE Seismic Research Review, Jackson Hole, Wyoming.

Rodi, W., E.R. Engdahl, E.A. Bergman, F. Waldhauser, G.L. Pavlis, H. Israelsson, J.W. Dewey, and M.N. Toksöz (2002). A new grid-search multiple-event location algorithm and a comparison of methods, *Proceedings*, 24th Annual Seismic Research Review, Ponte Vedra Beach, Florida, 403-411.

Rodi, W., S.C. Myers, and C.A. Schultz (2003). Grid-search location methods for ground-truth collection from local and regional seismic networks, *Proceedings*, 25th Annual Seismic Research Review, Tucson, Arizona.

Rodi, W. and M.N. Toksöz (2003). Confidence regions on seismic event locations based on multiple-event analysis, *Proceedings*, 25th Annual DoD/DOE Seismic Research Review, Tucson, Arizona, DOE NNSA.

Schultz, C.A., S.C. Myers, J. Hipp, and C.J. Young (1998). Nonstationary Bayesian kriging: a predictive technique to generate spatial corrections for seismic detection, location, and identification, *Bull. Seism. Soc. Am., 88*, 1275-1288.

Spencer, C. and D. Gubbins (1980). Travel-time inversion for simultaneous earthquake location and velocity structure determination in laterally varying media, *Geophys. J. R. Astr. Soc., 63*, 95-116.

Walter, W.R., K.D. Smith, J. L. O'Boyle, T.F. Hauk, F. Ryall, S.D. Ruppert, S.C. Myers, M. Anderson, and D.A. Dodge (2003), Improving the fundamental understanding of regional seismic signal processing with a unique western United States dataset, *Proceedings*, 25th Seismic Research Review, Tucson, Arizona.

Wilcock, W.S.D. and D.R. Toomey (1991), Estimating hypocentral uncertainties for marine microearthquake surveys: a comparison of the generalized inverse and grid search methods, *Marine Geophysical Researches, 13*, 161-171.